

# Swelling and Fracture of Bonded Rubber Spheres

K. A. MAZICH\* AND G. ROSSI

Polymer Science Department, Ford Motor Company, P.O. Box 2053, Drop 3198, Dearborn, Michigan 48121-2053

Received February 26, 1991;

Revised Manuscript Received May 14, 1991

Classically, the equilibrium swelling of elastomers is treated by balancing an osmotic force that favors expansion of the network with a retractive force produced by the stretching of elastically active chains in the network.<sup>1,2</sup> Network chains are free to swell until the equilibrium concentration determined by this balance is reached. At equilibrium, the deviatoric stress is zero and the concentration is uniform throughout.

Constraints within the network lead to different equilibrium states for the stress and concentration in the body of the swollen rubber. In particular, adhering one of the free surfaces of a rubber slab to a rigid substrate will hinder the swelling of network chains close to the bonded surface. In this case, the equilibrium concentration is smaller than in the free-swelling case and generally varies with position within the swollen network. Furthermore, nonzero stresses are present since dry-state dimensions must be maintained at the bonded interface. Detailed treatment of this class of problems has been given by Sternstein,<sup>3</sup> who modeled swelling of an infinite rubber matrix surrounding a rigid spherical inclusion, and Treloar,<sup>4</sup> who dealt with cylinders (of finite radius) bonded to a rigid core.

In this paper, we are principally interested in defining conditions for fracture that may result from the stress and strain in a constrained rubber specimen. Earlier studies, particularly work by Alfrey et al.,<sup>5</sup> have examined the effects of swelling and fracture in polymeric glass. Here, sharp interfaces between swollen sections and dry sections of the specimen produce stress that may exceed the tensile breaking stress of the material.

In this paper, first, we report the local variations of stress, strain, and composition (swelling ratio) for swollen rubber spheres bonded at the core to a rigid substrate. Here, the diffusion front is not sharp, in contrast to the case considered in ref 5. Much of the development parallels Treloar's<sup>4</sup> work for cylinders. Second, we use these classical results in conjunction with molecular theories of polymer fracture to define a fracture criterion. Our criterion is based on equilibrium calculations of stress and strain; the actual values of stress that develop during the process of swelling may exceed the values calculated in the equilibrium case. For this reason, our criterion provides only limiting conditions for fracture in swollen spheres.

We start with an unswollen sphere of radius  $a_0$  adhered to a rigid core of radius  $b_0$ . The radius of the swollen sphere at equilibrium is  $a$ . After swelling, principal extension ratios at radial position  $r$  are given by  $l_r$  in the radial direction,  $l_\theta$  in the  $\theta$  direction,  $l_\phi$  in the  $\phi$  direction. Extension ratios are based on the unswollen network. From symmetry,  $l_\theta = l_\phi$ . Boundary conditions are defined at the bonded surface between rubber and rigid core, where the tangential deformation is zero and  $l_\theta(r_0) = 1$ . Also, the radial component of stress,  $t_r$ , at the surface of the swollen sphere is zero.

The local swelling ratio,  $1/\nu$  (where  $\nu$  is the volume fraction rubber), is related to the principal extension ratios by

$$1/\nu = l_r l_\theta^2 \quad (1)$$

if we assume that the change of volume upon mixing is

zero and the swollen rubber is incompressible. Furthermore, the principal extension ratios are

$$l_r = \frac{dr}{dr_0} \quad l_\theta = l_\phi = \frac{r}{r_0} \quad (2)$$

Following Treloar,<sup>4</sup> eqs 2 can be rearranged to give

$$\frac{dl_\theta}{dr} = \frac{1}{r} \left( l_\theta - \frac{l_\theta^2}{l_r} \right) \quad (3)$$

A second differential equation for the radial variation of  $\nu$  is derived from thermodynamic and mechanical constitutive equations and the condition for mechanical equilibrium in the sphere. For a spherical geometry, the radial stress,  $t_r$ , and the tangential stress,  $t_\theta$ , at equilibrium satisfy

$$\frac{dt_r}{dr} = \frac{2}{r}(t_\theta - t_r) \quad (4)$$

Like Treloar,<sup>4</sup> we use results for a Gaussian network to relate stress and strain

$$t_\theta - t_r = \frac{\rho RT}{M_c} \nu (l_\theta^2 - l_r^2) \quad (5)$$

where  $\rho$  is the dry rubber density and  $M_c$  is the molecular weight between chemical junctions in the network. The addition of solvent to the network produces a stress along the principal directions of strain. For the radial stress, Treloar<sup>6,7</sup> derived

$$V_1 t_r = \frac{\partial G_m}{\partial n_1} + \frac{\rho RT}{M_c} \nu l_r^2 \quad (6)$$

where  $V_1$  is the molar volume of solvent,  $G_m$  is the free energy of mixing, and  $n_1$  specifies the moles of solvent.  $G_m$  is taken to have the usual Flory-Huggins form so that

$$\frac{\partial G_m}{\partial n_1} = RT(\ln(1-\nu) + \nu + \chi\nu^2) \quad (7)$$

where  $\chi$  is the solvent-polymer interaction parameter. Equations 4-6 lead to the second governing differential equation

$$\frac{d\nu}{dr} = \frac{2(1-\nu l_\theta^3)^2}{r \left( \nu^2 l_\theta^4 \left( A - \frac{B}{1-\nu} \right) - \frac{1}{\nu} \right)} \quad (8)$$

where  $A = 2\chi M_c/V_1$  and  $B = M_c/V_1$ . Equations 3 and 8 must be solved subject to the boundary conditions specified above. We used a standard relaxation procedure for two-point boundary value problems to solve these equations numerically.<sup>8</sup>

The constraint imposed by the rigid core on the swollen rubber produces a tensile stress in the radial direction. Our results for the radial tensile stress are shown in Figure 1 for a variety of "elastomers" that vary in cross-link density and, hence, in  $M_c$ . In the figure,  $M_c$  is represented as  $x$ , the number of equivalent steps along a network chain between chemical junctions. (By definition,  $x = M_c/\rho V_1$  where  $\rho$  is the dry polymer density and  $V_1$  is the molar volume of solvent.) Stress (the solid line in Figure 1) is plotted against the ratio of the radial distance,  $r$ , to the final total radius of the swollen sphere,  $a$ . The value of  $\chi$  is 0.41, but we have checked that the results are essentially unchanged for a range of  $\chi$  from 0.25 to 0.5. As shown, the maximum stress increases with decreasing  $x$ ; the material with  $x = 10$  has a maximum radial stress at the interface approximately 10 times greater than the

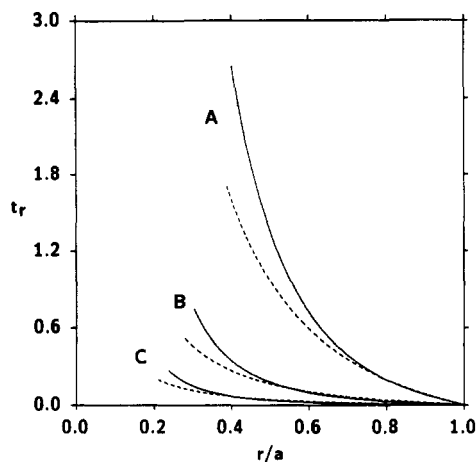


**Figure 1.** Stress in the radial direction in megapascals,  $t_r$ , plotted against  $r/a$  for  $x = 10$  (curve A), 100 (curve B), and 500 (curve C) and  $a_0/b_0 = 2$ . We chose  $\chi = 0.41$ ,  $\rho = 0.95$ , g/cm<sup>3</sup>,  $V_1 = 0.0894$  cm<sup>3</sup>/mol, and  $T = 298$  K (see ref 4). Solid lines represent spheres, and broken lines represent cylinders.

material with  $x = 500$ . Moreover, the thickness of the swollen material is greater in the latter case (as shown by the greater range of  $r/a$  in Figure 1), as expected for a more loosely cross-linked material.

Results for a cylindrical geometry (broken lines) with the same initial ratio,  $a_0/b_0$ , are also presented in Figure 1. A comparison of results for these geometries indicates that the swollen sphere presents greater stress to the material and a somewhat smaller swollen thickness for equal initial dimensions and network mesh size ( $x$ ).

Radial stress in swollen, constrained spheres is accompanied by compressive stress in the  $\theta$  (and  $\phi$ ) direction (not shown). This is due to the incompressible condition imposed on swollen rubber and the fact that swelling under constraint is smaller than free swelling. Like the radial tensile stress, the magnitude of the lateral compressive stress is greater at the rubber-core interface and decays to some smaller value at the outer surface of the sphere. The value of the compressive stress is not necessarily zero at the outer surface.

The calculated values for local stress and strain are used to define fracture criteria. As usual for elastomers, we follow the energy balance approach initiated by Griffith<sup>9</sup> and modified by Rivlin and Thomas.<sup>10</sup> These authors derived the energy release rate (per unit area),  $G$ , for a simple tension specimen with an edge crack

$$G = 2kWc \quad (9)$$

Here,  $W$  is the strain energy density in the bulk of the specimen (generally at equilibrium),  $c$  is the length of the crack, and  $k$  is a weak function of deformation approximately equal to  $\pi$ . Equation 9 is strictly applicable to specimens with through-the-thickness cracks. Although cracks will not (initially) run through the thickness of the sphere, we expect from dimensional arguments that the dependence on  $Wc$  will be the same. To continue our analysis, we identify  $c$ , with the length of the inherent cracks attributed to surface nicks, molding flaws, or cross-link density fluctuations. Gent<sup>11</sup> has reported that the effective size of these natural flaws is  $\sim 40$   $\mu$ m for many rubbers prepared with a variety of methods. As Gent<sup>11</sup> has noted, this value for  $c$  represents an apparent flaw size that reflects both the length and sharpness of the existing flaws.

Fracture criteria are defined by equating  $G$  to some critical value. For swollen rubber, we choose a critical  $G$  equal to the threshold fracture energy since only elastic

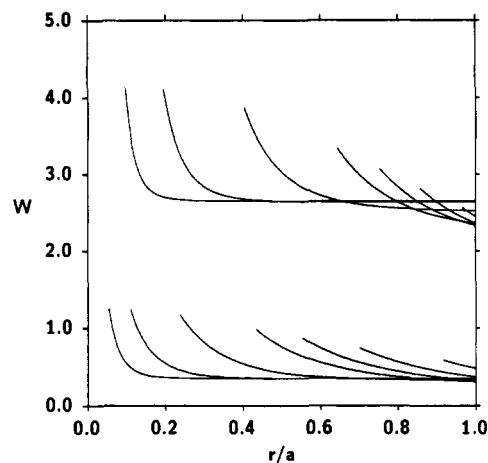


**Figure 2.** Strain energy density in megapascals  $W$ , plotted against  $r/a$  (same parameters as in Figure 1). The top set of curves correspond to  $x = 10$ , and the bottom set of curves correspond to  $x = 500$ . Curves from left to right in each set correspond to  $a_0/b_0 = 8, 4, 2, 1.4, 1.2, 1.1$ , and  $1.02$ , respectively.

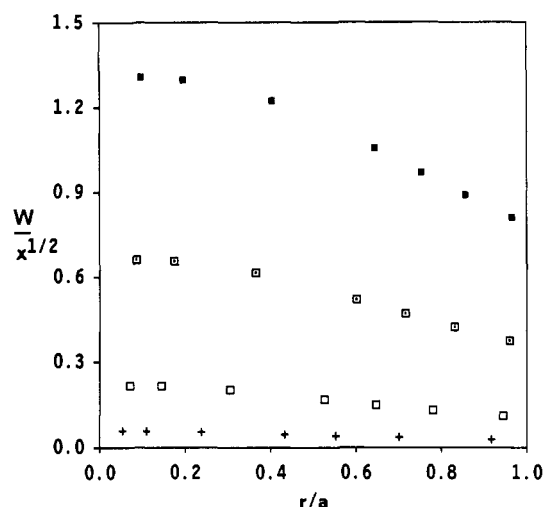


**Figure 3.** Maximum values of  $W/x^{1/2}$  plotted against  $r/a$  for  $x = 10$  (■), 25 (□), 100 (○), and 500 (+) and  $a_0/b_0 = 8, 4, 2, 1.4, 1.2, 1.1$ , and  $1.02$ . The critical value of  $W_c/x^{1/2} \sim 0.25$ .

processes contribute. The Lake-Thomas<sup>12</sup> theory relates the threshold fracture energy,  $G_0$ , to network characteristics as

$$G_0 = KM_c^{1/2} \quad (10)$$

where  $K$  is a constant specific to the polymer species in the network. This form for threshold fracture energy applies to rather tightly cross-linked networks such that  $M_c \leq M_e$ , the entanglement molecular weight.<sup>13</sup> Substituting eq 10 for  $G$  in eq 9 and rearranging, we expect fracture to occur when  $W$  is larger than some critical value,  $W_c$ , with  $W_c$  defined by

$$\frac{W_c}{x^{1/2}} = \frac{K(\rho V_1)^{1/2}}{2kc} \quad (11)$$

From our numerical solution, we calculate the strain energy density with the Gaussian form:<sup>7</sup>

$$W = \frac{\rho RT}{2M_c} (l_r^2 + 2l_\theta^2 - 3) \quad (12)$$

These results are plotted in Figure 2 for two networks ( $x = 10$  and  $x = 500$ ). The initial thickness of the rubber, expressed as  $a_0/b_0$ , is varied in each set of curves. As expected, the more tightly cross-linked network ( $x = 10$ )

yields a higher  $W$  and a smaller overall swelling (shown by the decreased range of  $r/a$ ). The figure also shows that thick shells of rubber bonded to the rigid core swell to a greater extent and attain higher strain energy densities. In addition, rubber located sufficiently far from the constrained interface in a thick shell may reach free-swelling equilibrium (shown by the horizontal sections in Figure 2).

In Figure 3, we plot the maximum values of  $W/x^{1/2}$ . When this quantity is larger than the critical value defined in eq 11, we expect that the network will fracture. We have written our criterion in this form to eliminate the dependence on the network mesh size. Values for the quantities entering eq 11 for a typical polymer-solvent system ( $K \sim 10^5 \text{ MPa}/(\text{g/mol})^{1/2}$ ,  $\rho V_1 \sim 10^2 \text{ g/mol}$ ,  $c \sim 0.04 \text{ mm}$ ) yield critical  $W_c/x^{1/2} \sim 0.25$ . In this case, a network with  $x = 500$  is apparently safe from fracture; the thicker shelled spheres for  $x = 100$ , i.e., for  $a_0/b_0 \sim 8$ , represent a borderline case. All geometries for  $x = 25$  and  $x = 10$  appear to fail according to this criterion.

The calculations presented in this paper give approximate conditions that are expected to result in failure. In fact, the actual stress, strain, and strain energy density experienced by the material during the process of swelling may exceed those for the equilibrium case. For this reason,

we expect our criterion to provide an upper limit for the onset of fracture.

**Acknowledgment.** We thank C. A. Smith for stimulating discussion and support of this work.

## References and Notes

- (1) Flory, P. J.; Rehner, J., Jr. *J. Chem. Phys.* **1943**, *11*, 521.
- (2) Flory, P. J. *Principles of Polymer Chemistry*; Cornell University Press: Ithaca, NY, 1953.
- (3) Sternstein, S. S. *J. Macromol. Sci.* **1972**, *B6*, 243.
- (4) Treloar, L. R. G. *Polymer* **1976**, *17*, 142.
- (5) Alfrey, T., Jr.; Gurnee, E. F.; Lloyd, W. G. *J. Polym. Sci.* **1966**, *C12*, 249.
- (6) Treloar, L. R. G. *Proc. R. Soc. London* **1950**, *A200*, 176.
- (7) Treloar, L. R. G. *The Physics of Rubber Elasticity*, 3rd ed.; Clarendon Press: Oxford, 1975.
- (8) Press, W. H.; Flannery, B. P.; Teukolsky, S. A.; Vetterling, W. T. *Numerical Recipes*; Cambridge University Press: Cambridge, 1986.
- (9) Griffith, A. A. *Philos. Trans. R. Soc.* **1920**, *A221*, 163.
- (10) Rivlin, R. S.; Thomas, A. G. *J. Polym. Sci.* **1953**, *10*, 291.
- (11) Gent, A. N. *Science and Technology of Rubber*; Eirich, F. R., Ed.; Academic Press: New York, 1978.
- (12) Lake, G. J.; Thomas, A. G. *Proc. R. Soc. London* **1967**, *A300*, 108.
- (13) Mazich, K. A.; Samus, M. A.; Smith, C. A.; Rossi, G. *Macromolecules* **1991**, *24*, 2766.